Observation and Characterization of Ferromagnetic Amorphous Nickel

J. M. Rojo,[1] A. Hernando,[1,2] M. El Ghannami,[2] A. García-Escorial,[3] M. A. González,[1]
R. García-Martínez,[1] and L. Ricciarelli[1]
[1]*Departamento Física de Materiales, Universidad Complutense, E-28040 Madrid, Spain*
[2]*Instituto de Magnetismo Aplicado UCM-Renfe, E-28230 Las Rozas, Madrid, Spain*
[3]*CENIM-CSIC, E-28040 Madrid, Spain*
(Received 2 January 1996)

Annealing an amorphous $Ni_{80}B_{20}$ alloy results in an intermediate state that is nanocrystalline with Ni_3B crystallites surrounded by an amorphous pure nickel phase. Amorphous nickel is found to be ferromagnetic with saturation magnetization about 60% of that of crystalline nickel and a Curie temperature around 60 K lower. By means of calorimetric measurements, a difference of energy of 0.028 eV atom^{-1} between amorphous and crystalline nickel is reported. [S0031-9007(96)00450-4]

PACS numbers: 75.50.Kj, 61.43.Dq, 61.46.+w

Amorphous alloys have unique properties that have encouraged numerous experimental studies on their characterization at an atomic scale [1]. They have also conveyed much theoretical interest, particularly in regard to magnetic properties. For amorphous pure metals in the transition series, a number of calculations have been carried out, often with controversial results; for example, in the case of amorphous nickel some authors predict ferromagnetic behavior [2], whereas others predict a nonmagnetic state [3]. So far, however, the preparation of pure amorphous metals has met insurmountable barriers and, in order to stabilize amorphous structures, transition metals require the presence at significant concentrations of, at least, a second component, often a metalloid [4]. In this Letter, we report the observation and characterization of a pure nickel amorphous phase, which is found to be ferromagnetic with a magnetic moment per atom about 60% of the corresponding value in the crystalline phase and a Curie temperature about 60 K lower. The amorphous nickel is formed after annealing an amorphous alloy of nominal composition $Ni_{80}B_{20}$. Annealing results in precipitation of boron as Ni_3B nanocrystals, whereas the excess nickel is left in the form of an amorphous nickel state. On an atomic scale, the structure of amorphous nickel resembles the so-called intercrystalline components of nanophases, which are currently the subject of much controversy [5,6]. Further annealing at a higher temperature results in a crystallization of amorphous nickel. The difference in energy per atom between the amorphous and crystalline phases has also been estimated by means of calorimetric measurements.

A rapidly solidified $Ni_{80}B_{20}$ (nominal composition) alloy was prepared by the melt spinning technique from a master alloy of the given composition melted in an induction furnace [1]. Samples were subsequently annealed, when necessary, in an argon atmosphere. Calorimetric measurements were carried out in a differential scanning calorimeter (DSC) operating at a fixed scanning rate. The x-ray diffractograms were obtained by using the copper $\lambda = 0.1541$ nm line, the effective angular resolution of the peaks being about 0.25 deg. Magnetic measurements were made in either a SQUID or a vibrating sample magnetometer. The thermal evolution of the alloy from its initial state is shown in the calorimetric curve of Fig. 1, obtained with a scanning rate of 10 K min^{-1}. Two very clear exothermic processes are observed, which peak, respectively, at 544 and 654 K. For a sample of 10.30 mg, the measured released heats were, respectively, -98.82 and -17.08 J g^{-1}. The two exothermic processes define three well differentiated states in the sample, which we shall denote in the following as *a*, *b*, and *c*, as shown in the figure.

The as-prepared sample (that we refer to as state *a*) was in the form of a homogeneous amorphous phase. Optical microscope observation showed at times the presence of a few micron-size crystallites. The x-ray diffractogram, Fig. 2(a), showed the two characteristic broad shoulders

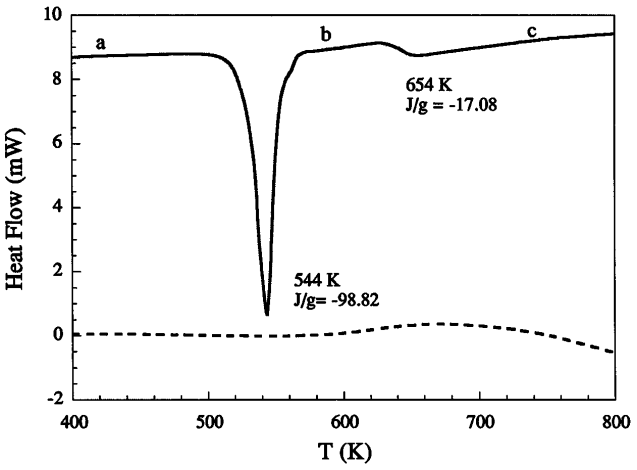

FIG. 1. Differential scanning calorimetry of an as-prepared $Ni_{80}B_{20}$ sample at a scan rate of 10 K min^{-1} (full line). The areas enclosed by each peak, in units of energy release per gram of sample, are shown in the figure. The two exothermic peaks separate states *a*, *b*, and *c*, as discussed in the text. For comparison, the response to a similar treatment of a $Ni_{75}B_{25}$ sample is shown (broken line). In both cases the base line was determined by subtraction of two successive runs.

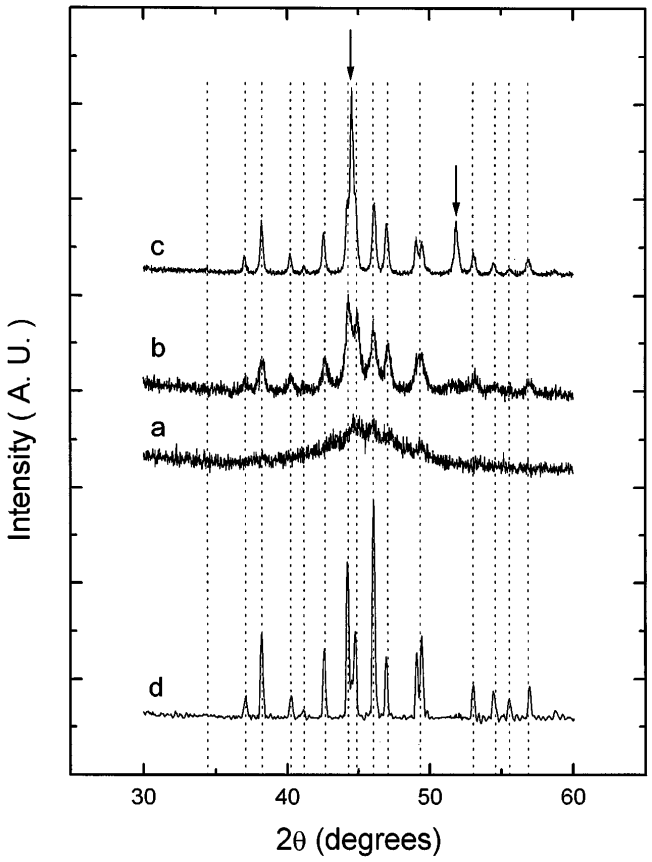

FIG. 2. X-ray diffraction patterns of an as-prepared sample (state *a*) and annealed samples for 1 h at 575 K (state *b*) and 825 K (state *c*). The dotted lines correspond to peaks that have been identified in terms of Ni_3B lines. The two arrows in stage *c* point to two peaks that correspond to nickel (111) and (200) reflections. X-ray wavelength $\lambda = 0.1541$ nm. For comparison, the diffraction pattern of a sample of $Ni_{75}B_{25}$ is shown as *d*.

of amorphous systems [7], the one centered around $2\theta = 45°$ being clearly visible in the range of the illustration.

Figure 2(b) shows the diffractogram corresponding to state *b*, after the first exothermic process. Comparing with the corresponding one in stage *a*, two main points are to be remarked: (i) A set of crystalline peaks appears. Bragg angles and intensities from the experiment were compared with standard ASTM card data of nickel, boron, and all their compounds (namely, Ni_3B, Ni_2B, and Ni_4B_3). Every measured peak was found to correspond to a Ni_3B line, and no line included in the card, with equal or larger intensity than the measured ones, was absent. In particular, no line that could possibly be associated to nickel was observed. We can safely conclude that *all* crystals in state *b* are Ni_3B. (ii) The two broad shoulders characteristic of state *a* (only the higher θ one is shown in the illustration) are still present, even if diminished with relation to the as-prepared sample. From the linewidths of the diffraction peaks [8], the average size of the Ni_3B crystallites was estimated, the result being 23 nm. Preliminary observations by means of high resolution transmission electron microscopy [9] confirm the presence of an extremely fine grained structure. These observations were checked by further preparing by the method described above for $Ni_{80}B_{20}$ a sample of nominal composition $Ni_{75}B_{25}$, which corresponds to the stoichiometry of the compound Ni_3B. Its diffractogram is shown as *d* in Fig. 2. It can be seen that there is a one-to-one correspondence between the lines in the *b* and *d* diffractograms. On the other hand, the base line is plane in *d*, indicating the absence of an amorphous phase.

A similar analysis for a sample in state *c* reveals important variations. In the x-ray diffractogram, shown as Fig. 2(c): (i) All the peaks interpreted before in terms of Ni_3B cristallites are still present, if somehow narrowed. (ii) There are two clearly defined new peaks that correspond to the (111) and (200) reflections of crystalline nickel. No other nickel line could be present in the range of θ's shown in the figure. (iii) The broad shoulders have completely disappeared, all the crystalline peaks lying now on a horizontal referential base line. A linewidth analysis, similar to the one described above, was performed, resulting in average values of the grain size of 36 nm for the Ni_3B crystallites and 40 nm for nickel.

We now describe the magnetic measurements. In the state *a* there is a residual magnetization of 1.5 emu g^{-1}. This value agrees very well with the previous work of Bakonyi, Panissod, and Hasegawa [10] in an alloy of similar composition. Their nuclear magnetic resonance and magnetic data are also consistent with our interpretation that the residual ferromagnetism is due to the contribution of small nickel particles, embedded in a paramagnetic amorphous matrix. On the other hand, both samples in states *b* and *c* are ferromagnetic, exhibiting clearly defined hysteresis loops as shown in the inset of Fig. 3. We have checked that, in agreement with earlier descriptions [10], our crystalline Ni_3B alloy is paramagnetic (a residual < 0.5 emu g^{-1} that we observe is thought to arise from nickel particles associated with inhomogeneities). It can, therefore, be concluded that all the ferromagnetism in states *b* and *c* is due to nickel. In the following, we shall restrict ourselves to magnetization measurements. Results connected with technical magnetism properties, which in nanocrystalline materials are known to depend dramatically on thermal treatments [11], will be the subject of a future publication [12].

From the hysteresis loops, the saturation magnetization of the sample M_s^* (hereafter, we shall use M_s^* to denote the magnetization referred to the mass of the whole sample to distinguish it from M_s, referred only to the nickel component) was measured after 1 h annealings at successively higher temperatures. The results are shown in Fig. 3. Two clear steps are visible which correspond to the onset of the states *b* and *c*. Since it has been shown recently [13] that about 6% of oxygen contamination can change up to 20% the saturation magnetization

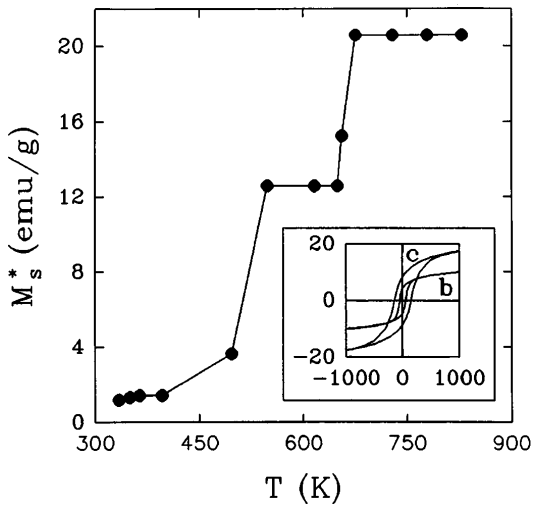

FIG. 3. Room temperature saturation magnetization M_s^* for samples treated for 1 h at the given temperature T. Notice the abrupt changes in M_s^* that can be related to the onset of states *b* and *c*. The inset shows typical hysteresis loops of the sample in state *b* and *c* in which M^*, in emu g^{-1}, is plotted as a function of H in Oe.

of nanocrystalline nickel, we have checked by Auger electron spectroscopy that no oxygen is detectable after removing by ion bombardment about a 100 nm layer from the surface. As our samples are 30 μm thick, we conclude that oxidation is not the cause of the low saturation magnetization of state *b*. The magnetic description of state *b* was completed by estimating its Curie temperature, as shown in Fig. 4, where the value of M_s^* is recorded as a function of temperature. The Curie temperature of state *b* extrapolates to 565 $\pm$ 20 K, whereas the one corresponding to state *c* is fully consistent with the crystalline nickel value of 627 K. Even though the rather extended tail in the amorphous sample suggests

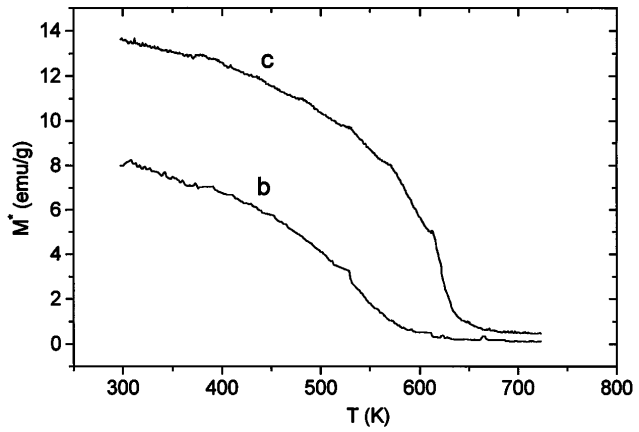

FIG. 4. Vibrating sample magnetometer measurements of magnetization M^* of samples in states *b* (interpreted as amorphous nickel) and *c* (crystalline nickel) as a function of temperature. Notice the two different values of the Curie temperature.

a certain distribution of nearest neighbor distances, it is clear that both *b* and *c* states are magnetically different.

There can be little doubt that the final state of the system (state *c*) is a mixture of Ni_3B and nickel crystallites. Both our x-ray measurements and predictions from the phase diagram of Ni-B agree on this point. Assuming that, in the state *c*, only crystalline nickel contributes to the saturation magnetization M_s^*, a simple estimation based on the nickel bulk value of $M_s = 54.4$ emu g^{-1} [14] leads to a value for the pure nickel fraction in the sample of $\alpha = 0.377$ g(Ni) g^{-1}(sample), which is equivalent to a real alloy composition of $Ni_{83}B_{17}$ (atomic). This difference can be accounted for by boron losses in the preparation process from the initial products concentrations of 80% $-$ 20%.

We claim that state *b* consists of a nanocrystalline phase of Ni_3B surrounded by amorphous nickel. We make this claim mainly on the grounds that no crystalline x-ray peaks, other than those pertaining to Ni_3B, are visible and that in state *b* we have a well-defined ferromagnetic state. As is well known, nickel is a strong itinerant ferromagnet that loses this property once it is alloyed with boron because the excess electrons fill the minority band. Once boron is precipitated to form the Ni_3B crystals, the nickel band becomes unbalanced again, even if a slightly different atomic environment, due to the amorphous linkage, results in a lower saturation magnetization. Also, the decrease in Curie temperature can be thought of in terms of a slight modification in the neighbors bonding. As the x-ray diffractogram from state *c* has a zero base line, we can safely conclude that all the nickel that was in the amorphous phase in state *b* transforms into crystalline nickel in state *c*. We shall, therefore, use the above value of α for the fraction of amorphous nickel in state *b*. By taking the experimental value of $M_s^* = 12.4$ emu g^{-1} (sample) in state *b* (Fig. 3), we obtain the saturation magnetization of the amorphous nickel as $M_s = \alpha^{-1} M_s^*$. The resulting value of $M_s = 32.9$ emu g^{-1} is about 60% of the corresponding value in the bulk crystal. The main source of error of this value arises from neglecting the residual M_s that appears in state *a*. Had the latter been due to nickel crystallites, the computed fraction of nickel in amorphous state in *b* would decrease, and the resulting value of M_s in the amorphous state would also decrease by about 5%.

Although no direct measurement has been made, we believe that the presence of boron in the amorphous component of state *b* is difficult to reconcile with the existence of a well-defined second peak in the DSC curve. We now present additional evidence that the amorphous component of phase *b* is just nickel. If this amorphous component contained a sizable amount of boron, the total volume of Ni_3B in the sample would have to increase from *b* to *c* as the excess boron precipitated in Ni_3B crystals. In order to check this possibility, we have compared the *integrated intensities*, i.e., *areas* of the Ni_3B

x-ray lines in both the *b* and *c* states and found within experimental error to remain *unchanged.* Ni_3B lines, as indicated above, become more intense and narrow (probably due to grain coalescence), but the fact that their areas remain constant ensures that no more Ni_3B is formed in *c*. Undoubtedly, when we say that in state *b* the amorphous component is just nickel, we cannot exclude a tiny amount of boron to be present (even in equilibrium, crystalline nickel admits about 0.3% boron at room temperature), but the above comparison of areas allows one to set an upper limit of 2%. Even at this level, boron would work as an impurity rather than as a stabilizing second component, as it is currently admitted that at least around 17% boron is required to stabilize amorphous phases [1,10].

Explaining why a given structure is preferred by a particular system is one of the key issues in materials science, although comparing total energies for two different possible structures is one of the most demanding computations of solid state theory [15]. Moreover, experimental investigation of energy differences is an obviously difficult task, as it requires the preparation of metastable structures with long relaxation times. Only recently have the surface energy differences between two different reconstructions of the same surface been measured [16]. We propose here that our DSC data can be used to calculate the difference in energies per nickel atom, ΔE, in the amorphous, E_{amor}, and crystalline, E_{crys}, phases. From those data (Fig. 1), we obtain a value of the released heat across the second peak of $\Delta E^* = -17.08\ \mathrm{J\,g^{-1}}$ (sample), where we have again denoted by starred symbols those relating to the *sample* as a whole. According to our previous discussion, this heat is released as the amorphous nickel transforms into the crystalline phase. It is worth remarking that the use of magnetic data results in a very accurate determination of the fraction of nickel that evolves from one state to the other. Using again the value of *a* as above, we obtain $\Delta E = \alpha^{-1}\Delta E^*$, which leads to an atomic value of

$$\Delta E = 45.3\ \mathrm{J\,g^{-1}}\ (\mathrm{nickel}) = 0.028\ \mathrm{eV\,atom^{-1}}.$$

The estimated error is $+8\%$, arising from the same source as indicated in relation to the M_s determination for the amorphous nickel. The value of ΔE is a direct experimental determination of the energy difference between two structures of a pure metal. It is of the order of the calculated differences between the energies of two different compact structures [17], and also of the order of the stacking fault energy [18]. This seems to suggest that, in our system, atomic evolution from the amorphous to the crystalline structure of nickel does not involve much rearrangement in first neighbor bonds.

It is tempting to compare our system with the nanophases of copper or iron obtained by high temperature compaction. The low value that we obtain for ΔE seems to suggest that the structure that we interpret as amorphous nickel is not related to the one corresponding to the so-called anomalous boundaries [5], which are characterized with a much lower density. On the other hand, the fact that our amorphous structure further transforms into a crystalline one clearly shows that the material that fills in the region between the Ni_3B crystallites in state *b* is very different from normal crystal boundaries [6]. Although, at first sight, our material in state *b* resembles the intercrystalline component of nanophases, we conclude that its structure is quite different and can be better described in terms of an amorphous phase with short range order.

In summary, following annealing of an initially amorphous Ni-B alloy, we have identified a pure nickel amorphous phase, which contains the excess nickel that is left after precipitation of Ni_3B crystallites. This amorphous phase cannot be described in terms of either anomalous or standard grain boundaries and has an energy of about 28 $\mathrm{meV\,atom^{-1}}$ higher than the crystal. First neighbor bonding is similar in both amorphous and crystalline phases. The nickel in the amorphous phase is found to be ferromagnetic with M_s equal to 60% of that of crystal nickel and a Curie temperature about 60 K lower.

Discussions with A. R. Yavari are gratefully acknowledged. A. H. thanks the Spanish CICYT for financial support.

[1] *Rapidly Solidified Alloys*, edited by H. H. Liebermann (M. Dekker, New York, 1993).
[2] M. Liebs, K. Hummler, and M. Fähnle, Phys. Rev. B **51**, 8664 (1995).
[3] M. Yu and Y. Kakehashi, Phys. Rev. B **49**, 15 723 (1994).
[4] T. Egami and Y. Waseda, J. Non-Cryst. Solids **64**, 113 (1984).
[5] S. Trapp, C. T. Limbach, U. Gonser, S. J. Campbell, and H. Gleiter, Phys. Rev. Lett. **75**, 3760 (1995).
[6] E. A. Stern, R. W. Siegel, M. Newville, P. G. Sanders, and D. Haskel, Phys. Rev. Lett. **75**, 3874 (1995).
[7] T. Egami, in *Glassy Metals I,* edited by H. J. Guntherodt and H. Beck (Springer-Verlag, Berlin, 1981), p. 25.
[8] L. V. Azaroff, *Elements of X-Ray Crystallography* (McGraw-Hill, New York, 1968), p. 557.
[9] C. Ballesteros (private communication).
[10] I. Bakonyi, P. Panissod, and R. Hasegawa, J. Appl. Phys. **53**, 7771 (1982).
[11] A. Hernando, M. Vázquez, T. Kulik, and C. Prados, Phys. Rev. B **51**, 3581 (1995).
[12] A. Hernando *et al.* (to be published).
[13] H. Kisker, T. Gessmann, R. Würschum, H. Kronmüller, and H. E. Schaefer, Nanostruct. Mater. **6**, 925 (1995).
[14] S. Chikazumi, *Physics of Magnetism* (Krieger, Malabar, 1978), p. 19.
[15] M. C. Payne, M. P. Teter, D. C. Allan, A. A. Arias, and J. D. Joannopoulos, Rev. Mod. Phys. **64**, 1045 (1992).
[16] Y. Y. Yeo, C. E. Wartnaby, and D. A. King, Science **268**, 1731 (1995).
[17] T. Asada and K. Terakura, Phys. Rev. B **47**, 15 992 (1993).
[18] F. R. N. Nabarro, *Theory of Crystal Dislocations* (Dover, New York, 1987), p. 251.